Finite Element Method Based Technical Investigation of ICEV Chassis with EV Conversion Module

Sadixhya Pandey[1], Shubhanjan Dhoj Joshi[1], Abhishek Karki[1], Angel Gurung[1], Rohit Sapkota[1], Sirapa Shrestha[*1,2], Asbina Baral[4], Sailesh Chitrakar[1,3]

[1]Department of Mechanical Engineering, Kathmandu University, Nepal
[2]Project 22-05 Laboratory, Kathmandu University, Nepal
[3]Turbine Testing Laboratory, Kathmandu University, Nepal
[4]Ministry of Education, Science and Technology, Government of Nepal
[*1,2]sirapa.shrestha@ku.edu.np

Received: 14 April 2025; Revised: 9 June 2025; Accepted: 10 July 2025, Published:17 August 2025

Abstract

Nepal is shifting towards cleaner and sustainable means of transportation through import of electric vehicles and conversion of conventional vehicles into electric. The conversion process requires static and dynamic analysis of vehicle chassis to ensure structural integrity. This study aims to assess static structural performance of a conventional car model that is the brink of 20-year age limit. CAD modelling is done using SolidWorks and Finite Element Analysis is done in ANSYS on the chassis of a Maruti 800 model with electric retrofitting components. The study carries out on-field measurements and literature review to gather vehicle specifications, and defines simulation variants related to chassis material and configuration of battery and motor. The materials considered are carbon fiber, high-strength steel, low alloy normalized steel 4140, and aluminum alloy wrought 6061. A total load of 5,405.36 N was applied on different placement configurations of motor and battery: front, trunk, motor in front, battery in front, motor in trunk, battery in trunk, motor in front with battery at the bottom, and motor in trunk with battery in front. The ultimate stresses for the varied materials employed in this study for the chassis falls within the range of 3-12 MPa, all well below the allowable stress range of 104-1470 MPa. It can be inferred that the selected materials exhibit a high degree of safety for the structural integrity of the vehicle's chassis. Based on the simulation results, the optimal placement for the motor and battery is found to be at the front of the chassis. Additionally, low alloy steel stands out as the safest material choice for the chassis. The results stand out by addressing Nepal specific transportation needs and offering a comparative material performance analysis tailored for EV retrofitting in low-to-mid-income economies. The study underscores the need for identifying minimal stress conditions for maximum load capacity, and can be used as an important component to form guidelines for vehicle conversion in Nepal.

Key Words: *Vehicle Conversion, Finite Element Analysis, Static Structural Analysis, Maruti 800, Component Placement, Nepal*

1. INTRODUCTION

Transportation sector of Nepal is determined to shift towards electric as confirmed by the first and the second Nationally Determined Contributions (NDCs) submitted by the country (GoN, 2016, 2020). The latest NDC has set targets for 2025 and 2030 to increase share of Electric Vehicles (EVs) both in private and public fleets to reduce demand of fossil fuel and subsequent emission as shown in Table 1. According to Department of Customs, EV imports account for one-third of the market share in terms of value for the current fiscal year (Prasain, 2024). After the Ministry of Physical Infrastructure and Transport decided to allow modifications of existing vehicles in 2022 ("Government to Allow Conversion of ICE Vehicles into Electric or Other Alternative Fuel Vehicles," 2022), multiple organization have begun to conduct research and projects to convert old Internal Combustion Engine Vehicles (ICEVs) into electric.

Table 1. *Second NDC targets of Nepal for the period of 2021-2030.*

Target Year	2025	2030
Target Share of EVs		
Private Vehicles	25%	90%
Public Vehicles	20%	60%
Fossil Fuel Demand		
Approximate Projection (Business As Usual)	40 million GJ	48 million GJ
Targeted Reduction	9%	8%
Emission		
Approximate Projection (Business As Usual)	2,988 Gg CO_2 eq.	3,640 Gg CO_2 eq.
Targeted Reduction	8%	28%

Conversion of an ICEV to EV requires

replacement of fuel system, air filter, exhaust system, and engine components with equivalent or desirable electrical components. While transmission, clutch and drivetrain can be utilized, space availability and structural ability of chassis should be considered in the design phase (Liu et al., 2005). This paper aims to conduct static structural analysis of a conventional car chassis with electric retrofitting.

2. LITERATURE REVIEW

Static structural analysis of a vehicle chassis helps to ensure ability of the chassis to withstand external and internal stresses and forces without fracture or failure. Multiple studies have used Finite Element Analysis (FEA) to conduct static structural analysis of different types of vehicles.

A study conducted structural analysis on different scooter chassis frames to determine stress and deformation induced under different loading conditions using Finite Element Analysis (FEA). It also identified failure modes through modal analysis. Materials and associated mechanical properties were varied for the analysis. Critical stress areas were determined and a frame structure, safe under the applied shear stresses, was designed. Elliptic cross section was found to increase vertical stiffness and put lateral stiffness in acceptable range (Balaguru et al., 2019).

Another study focused on optimizing structural design of a scooter frame using FEA. A 3D model was created using Pro-E software and Hyper Mesh was used to crease mesh. It comprehensively conducted comparative analysis to evaluate the structure, section shapes, load attributes, and metallurgical and mechanical properties of the components. Modal analysis was conducted to identify different mode shapes and natural frequencies to understand dynamic behaviour of the frame. It also assessed the frame's performance against industry standards and analogous products (Poudel & Button, 2018).

Another study also conducted modal analysis to identify failure modes in a scooter chassis. It validated the frame, identified critical stress and evaluated safety under different loading conditions (Shiva Prasad et al., 2020).

A set of studies have conducted structural analysis on truck chassis as well. A study applied different loading and boundary conditions on a truck chassis by rigidly fixing both of its rear and front ends. It simulated real-world scenarios and comprehensively analysed the structural response for static loading conditions. The maximum deformation occurred at the middle position of the frame, indicating a point of vulnerability or potential stress concentration. Minimum deformation was seen at the two fixed supports, suggesting these locations as points of structural stability and resilience (Journal & Engineering, 2013).

Similar static analysis was conducted in which real-world conditions and stressors were replicated. The chassis exhibited a multifaceted range of behaviours, influenced by a combination of operational load scenarios and internal factors. This observation underscored the complexity of the interactions within the structural components of the truck body, highlighted the need for a comprehensive understanding of both external and internal factors in assessing its performance and durability (M.B. Liu a 1, W.P. Xie b, n.d.).

Shifting from conventional vehicle to electric requires weight optimization to increase overall efficiency. The chassis frame has to provide structural safety to the vehicle and also incorporate different subsystem of the vehicle.

A study conducted on a bus chassis focused on replacing steel frames with aluminum alloys without compromising vehicle safety and strength. After replacing chassis frame with aluminum 6062-T6 and aluminum 7075-T6 weight reduction of 65.61% and 64.33% was achieved respectively. Structural analysis revealed that the new frames did not exceed their respective Ultimate Tensile Strength thus making the design frame safe. Aluminum 7075-T6 frame exhibited lesser stress and deformation than the other alloys making it an optimum material for the chassis frame (Nandhakumar et al., 2020).

Similar study evaluated existing electric bus chassis frame and identified specific steel members suitable for replacement. Next, a careful selection of potential aluminum alloys were made based on weight and mechanical properties. It redesigned the chassis frame to ensure a balance between weight reduction and the preservation of safety and strength characteristics. A thorough comparison of the simulation results was conducted to assess the viability and effectiveness of the weight optimization strategy (Rajappan & Vivekanandhan, 2013).

Another study assessed behavior tendency of alternative urban vehicle under externals loads and internal factors to ensure that the chassis can accommodate static loads. Three different

materials were selected: carbon steel, aluminum 6061 and carbon fiber reinforced plastic. The chassis varied the thickness as 1.2 mm, 1.4 mm and 0.9 mm. Static analysis revealed that carbon steel's chassis was the strongest for the least thickness (Ary et al., 2020).

These studies have emphasized balancing structural strength, enhancing load-bearing capacity and improving overall structural performance of different vehicles. Converting an existing chassis of conventional vehicle to electric requires consideration of weight distribution, material consideration and chassis thickness to improve structural integrity.

3. METHODOLOGY

The method employed in this study is shown in Figure 1. Each of the steps are described in the sub-sections below:

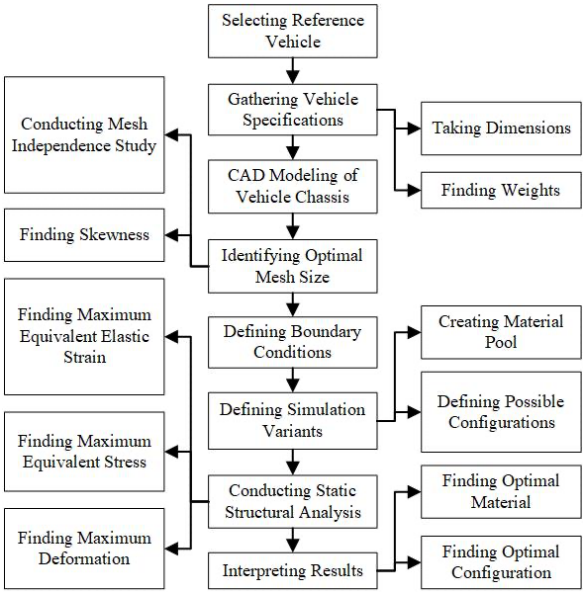

Fig.1: *Methodology of the Study.*

3.1 Selection of Reference Vehicle

Maruti 800 was chosen for this study to conduct static structural analysis. It is commonly used for taxi service in Nepal, and is in the brink of 20-year age limit, with potentially compromised physical status. Department of Transport Management under the Ministry of Infrastructure and Transport had decided in 2018 to place ban on vehicles older than 20 years (Ojha, 2018). Maruti 800 is a compact and lightweight model with simple mechanical and electrical system. The layout facilitates integration of electric motor, battery pack and associated control systems without major modifications in the vehicle structure. The spare parts are readily available due to its widespread usage and it has smaller engine and lower power requirements.

3.2 Collection of Vehicle Specifications

Maruti 800 has a monocoque chassis manufactured using normalized low alloy steel. Dimensions associated with wheelbase, length, width, height, front track width, rear track width, ground clearance, curb weight and gross vehicle weight used for CAD modeling are given in Table 2. The weights of different components used for the study are shown in Table 3.

Table 2. *Vehicle specifications.*

Parameters	Values	Remarks
Wheelbase	2,175 mm	On-site measurement
Length	3445 mm	On-site measurement
Width	1515 mm	On-site measurement
Height	1475 mm	On-site measurement
Front track width	1215mm	On-site measurement
Rear track width	1215mm	On-site measurement
Ground clearance	160 mm	On-site measurement
Curb weight	650 kg	(*Maruti 800 Tech Detailing*, n.d.)
Gross vehicle weight	2,000 kg	

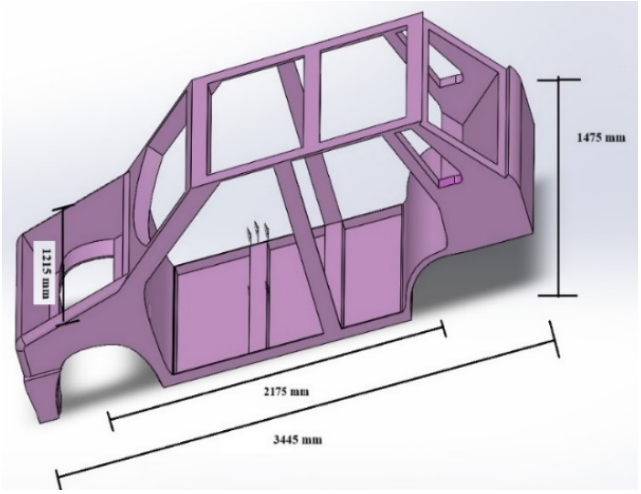

Fig.2: *Measurements using CAD model.*

Table 3. *Loading conditions.*

Parameters	Values	Assumptions
Battery	1226.3 N	Li-$FePO_4$ 12 KWh ("LiFePO4 vs. Lithium Ion Batteries: What's the Best Choice for You?," n.d.)
People	2746.8 N	5 people 75 kg each
Motor	255.06 N	Permanent Magnet Synchronous Motor,10 KW,72 V (*Permanent Magnet Synchronous Motor (PMSM) Contro*, n.d.)
DC-DC Converter	14.789 N	72-12V, 500 W(*Fully Isolated Heavy Duty Industrial and Military Grade 72VDC to 12VDC and 24VDC DC/DC Converters 40 Amp, 540 Watt. 5 Year Warranty.*, n.d.)
Controller	27.86 N	72 V / 400 A, IP 67 (*72 Volt Electric Scooter Speed Controllers - ElectricScooterParts.Com*, n.d.)
Total Weight	4,242.95 N	

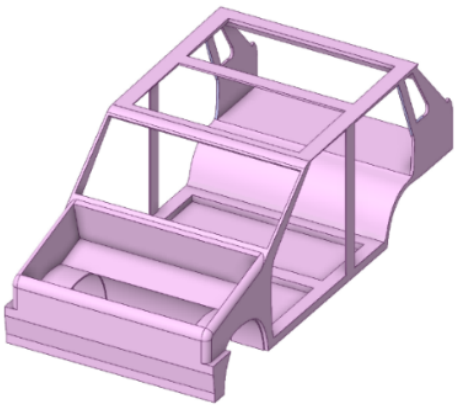

Fig. 3: *CAD model of chassis of Maruti 800.*

3.3 Identifying Optimal Mesh Size

A mesh consists of discrete individual elements that approximates a geometry. A mesh is considered to be of higher quality is it improves either time to convergence or stability or accuracy without affecting other parameters negatively (*Mesh Quality: Mesh Visualization Tips*, n.d.). Here, mesh independence study was carried out followed by determination of skewness. Skewness is the deviation between the optimal cell sizes to the existing cell size. A skewness of 0 corresponds to ideal mesh and that of 1 corresponds to the worst (*Mesh Quality: Mesh Visualization Tips*, n.d.). A graph of mesh size vs. total deformation was plotted as shown in Figure 4 until a constant value of total deformation was reached. An optimal element size of 12 mm was determined electing a skewness value of 12 mm in structural analysis helps keep the computer simulations stable and accurate. It means the software is using a balanced and well-arranged grid to better understand how structures respond to forces, making the results more trustworthy. Similarly, figure 3 shows bar graph showing element metrics and number of elements for 12 mm element size.

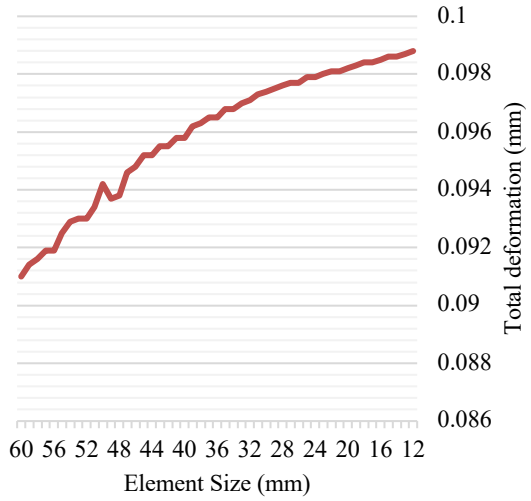

Fig. 4: *Plot showing mesh independence study.*

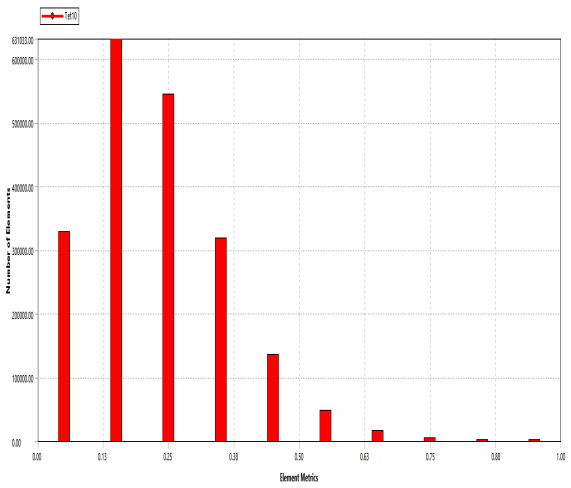

Fig. 5: *Graph of number of elements vs. element metrics.*

The final meshed model is shown in Figure 6.

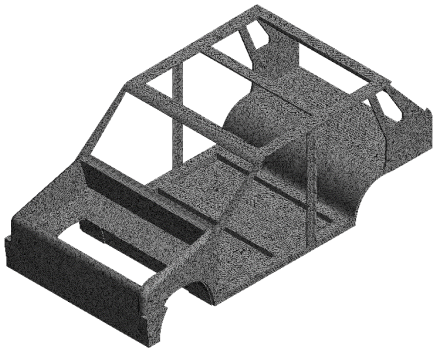

Fig. 6: *Meshed model for simulation.*

3.4 Defining Boundary Conditions

As monocoque chassis is stiff, it is capable of absorbing all static and dynamic loads with deflections that are low in comparison to the deflections that occurs at suspension. The chassis is fixed at the front and rear suspension, and loads are vertically applied on the geometry (Figure 7). Loading conditions for battery (1226.3 N), three passengers and one driver (3924 N), motor (255.06 N), DC-DC converter (14.789 N) and controller (27.86 N) were defined. The battery was placed at the bottom of the chassis in one case and at the trunk space in other case.

Fig. 7: *Bottom view of chassis showing fixed support.*

3.5 Simulation Variants

This study considered high strength steel, aluminum and carbon fiber for comparison. The properties of all these materials as given in Table 4. The value of Factor of Safety is taken as 3 (*ANSYS SIMULATION SOFTWARE*, n.d.) to find allowable stress values for low alloy normalized steel 4140 (*AISI 4140 Alloy Steel: Fushun Special Steel Co., Ltd. - Professional Supplier of Special Steel, and Manufacturer of Tool Steel*, n.d.), high strength steel (Helal et al., 2018), Aluminum alloy, wrought 6061 (Ary et al., 2020) and Carbon fibre (Ary et al., 2020).

Table 4. *Properties of different materials.*

Parameters	Low alloy normalized steel 4140	High strength steel	Aluminium alloy, wrought 6061	Carbon fibre
Tensile strength	655 MPa	345 MPa	313.1 MPa	577 MPa
Yield strength	415 MPa	207 MPa	259.2 MPa	300 MPa
Bulk modulus	140,000 MPa	1.75×10^{-5}MPa	67686 MPa	90372 MPa
Shear modulus	80,000 MPa	80769 MPa	25955 MPa	53000 MPa
Young's modulus	$1.9\times 10^5 - 2.1\times 10^5$MPa	$2.1x10^5$ MPa	69040 MPa	$1.33x10^5$ MPa
Poisson's ratio	0.27 - 0.30	0.30	0.33	0.25472
Ultimate stress	1015 MPa	345 MPa	313.1 MPa	4410 MPa
Allowable Stress	338.33 MPa	115 MPa	104.36 MPa	1470 MPa

The placements of battery and motor was varied as given below (Figure 8) for the simulation:

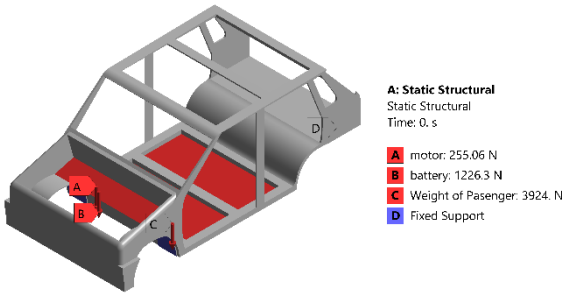

Fig. 8(a): *Case I: Motor and battery at the front.*

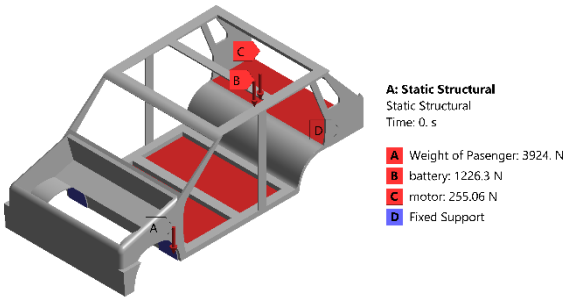

Fig. 8(b): *Case II: Motor and battery in the trunk.*

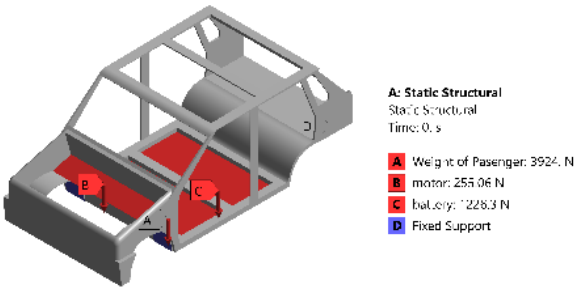

Fig. 8(c): *Case III: Motor at the front and battery at the bottom.*

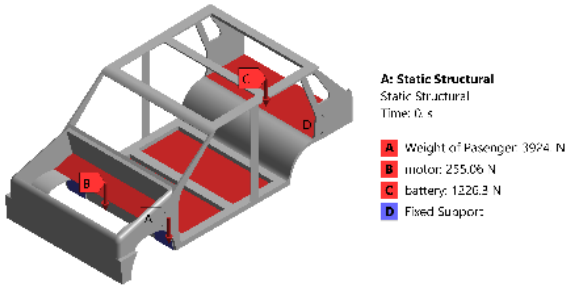

Fig. 8(d): *Case IV: Motor at the front and battery in the trunk.*

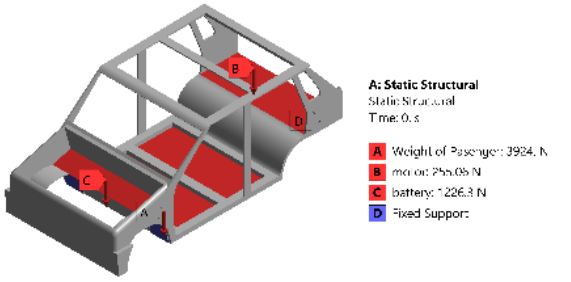

Fig. 8(e): *Case V: Motor at the trunk and battery at the front.*

3.6 Conducting static structural analysis

Table 6. *Interpretation of values of normalized equivalent stress.*

Range	Interpretation
0 - 0.5	Low stress level, considered safe for most applications
0.5 - 0.8	Moderate stress level, approaching the yield point, might require caution and design optimization
0.8 - 1.0	High stress level, close to failure, potentially unsafe and requiring immediate attention.

Equivalent elastic strain, equivalent stress, and total deflection and normalized equivalent stress were found out. The normalized equivalent stress which is the ratio of equivalent stress to ultimate tensile stress is used to show if the structure is safe.

4. RESULTS AND DISCUSSION

The results obtained for different cases are given below.

4.1 Case I: Motor and Battery at the Front

In the interaction between the battery and motor at the front, the materials exhibit distinct stress levels numerically, with aluminum leading at a maximum equivalent stress of 3.8056 MPa. High-strength steel follows with 3.8536 MPa, low alloy steel with 3.9221 MPa, and carbon fiber with 4.1565 MPa (Figure 9).

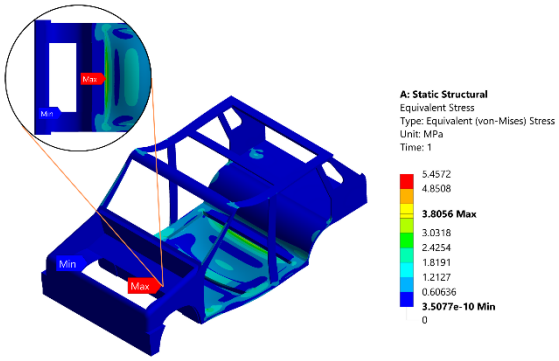

Fig. 9(a): *Aluminum.*

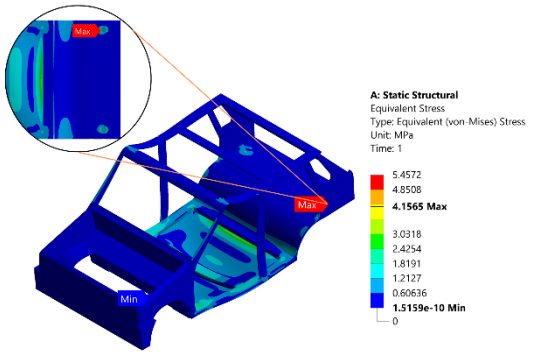

Fig. 9(b): *Carbon Fibre.*

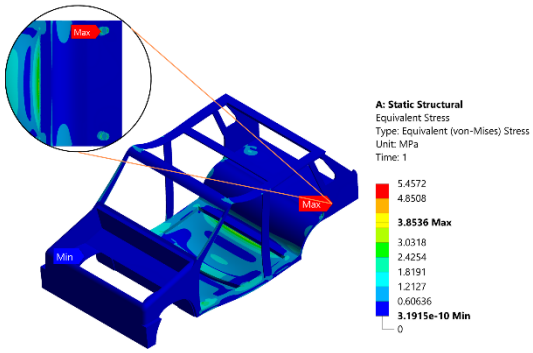

Fig. 9(c): *High Strength Steel.*

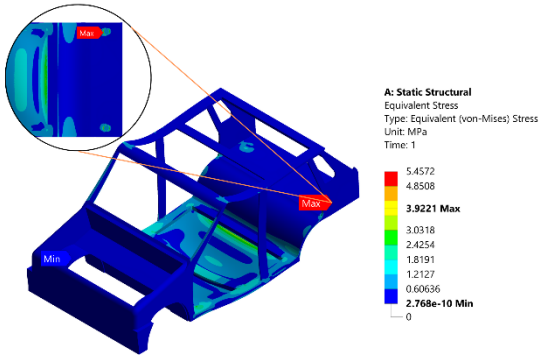

Fig. 9(d): *Low Alloy Steel.*

Low alloy steel shows the least total deformation with 0.074455 mm, emphasizing its structural suitability. The distinct total deformation values for other materials are as follows: High-strength steel - 0.075265 mm, Aluminum - 0.22807 mm, Carbon fiber - 0.11927 mm (Figure 10).

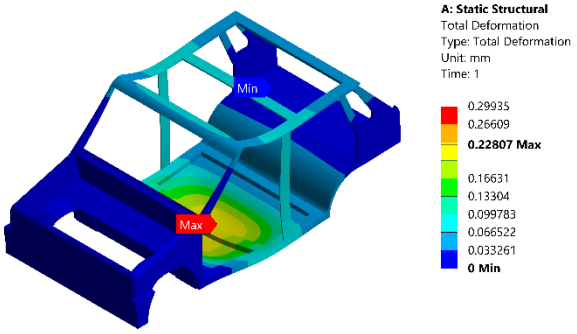

Fig. 10(a):. *Aluminum.*

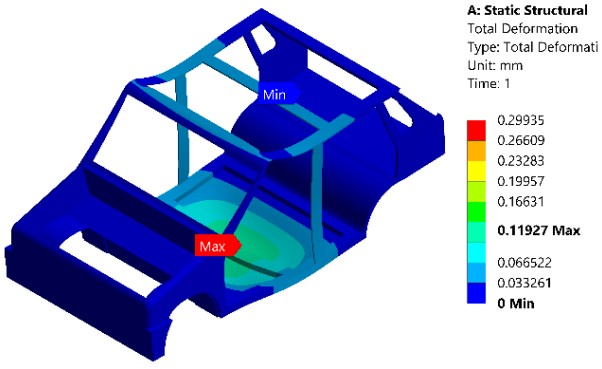

Fig. 10(b): *Carbon Fiber.*

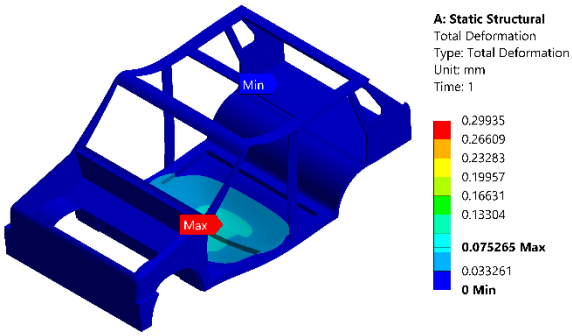

Fig. 10(c): *High Strength Steel.*

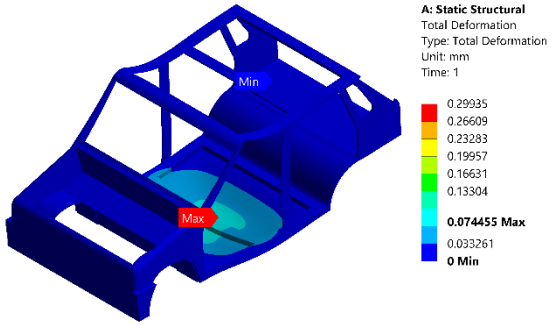

Fig. 10(d): *Low Alloy Steel.*

4.2 Case II: Motor and Battery in the Trunk

Analyzing the battery and motor trunk interaction, aluminum showcases the highest stress levels numerically, with a maximum equivalent stress of 4.5694 MPa. High-strength steel follows with 4.8119 MPa, low alloy steel with 4.8901 MPa, and carbon fiber with 5.1569 MPa (Figure 11).

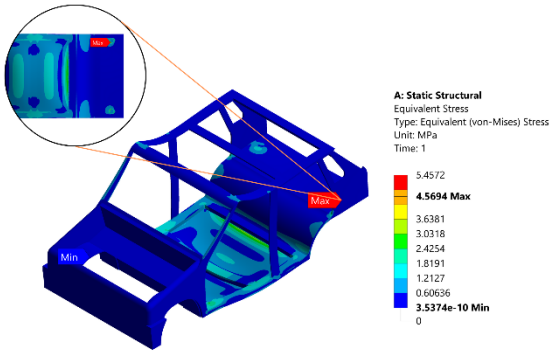

Fig. 11(a): *Aluminum.*

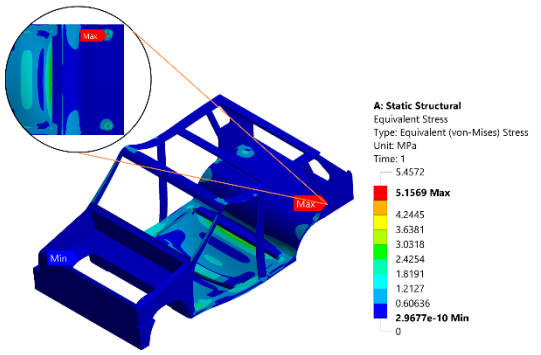

Fig. 11(b): *Carbon Fiber.*

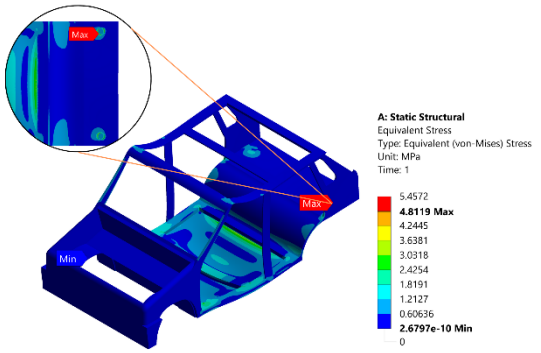

Figure 11(c): *High Strength Steel.*

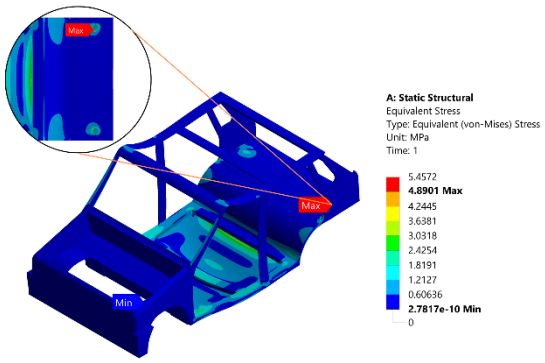

Figure 11(d):. *Low Alloy Steel.*

Low alloy steel shows the least deformation 0.0756503 mm, reinforcing its effectiveness in this particular structural configuration. The distinct total deformation values for other materials are as follows: Aluminum - 0.23176 mm, Low alloy steel - 0.075685 mm, Carbon fiber - 0.12127 mm (Figure 12).

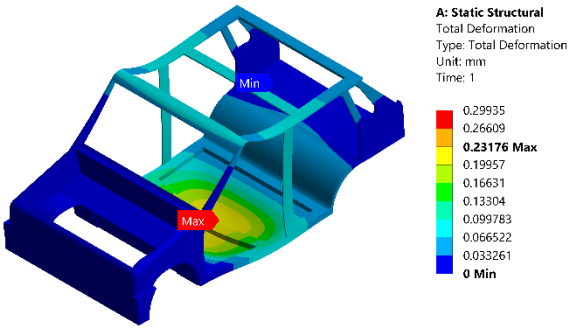

Fig. 12(a): *Aluminum.*

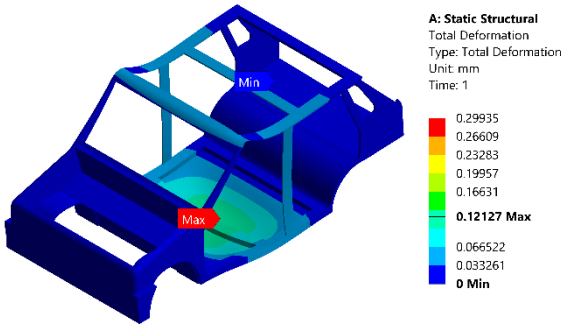

Fig. 12(b): *Carbon Fiber.*

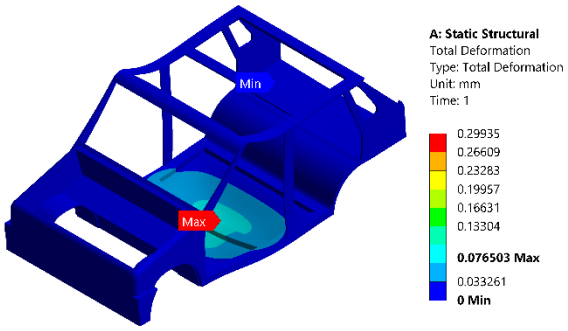

Fig. 12(c): *High Strength Steel.*

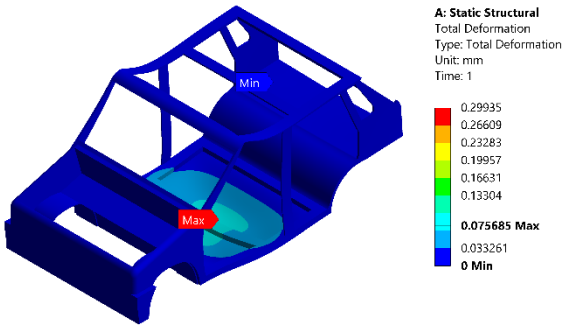

Fig. 12(d): *Low Alloy Steel.*

4.3 Case III: Motor at the Front and Battery at the Bottom

In the interaction between the motor front and battery bottom, aluminum once again outperforms with the highest stress levels numerically, reaching a maximum equivalent stress of 4.999 MPa. High-strength steel follows with 5.1495 MPa, low alloy steel with 5.4572 MPa, and carbon fiber with 4.1565 MPa (Figure 13).

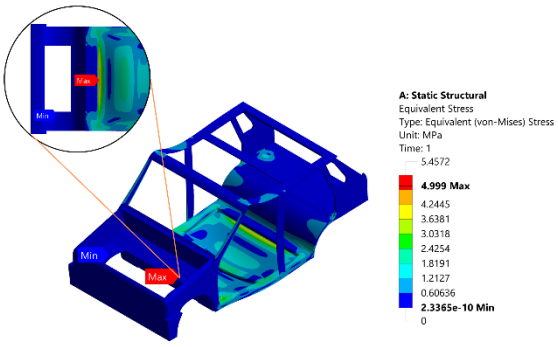

Fig. 13(a): *Aluminum.*

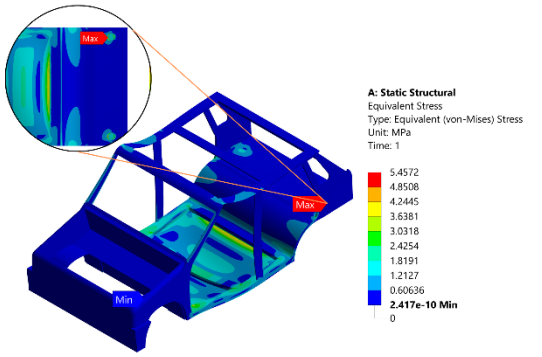

Fig. 13(b): *Carbon Fiber.*

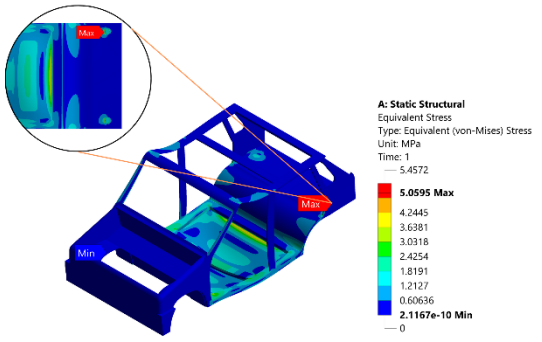

Fig. 13(c): *High Strength Steel.*

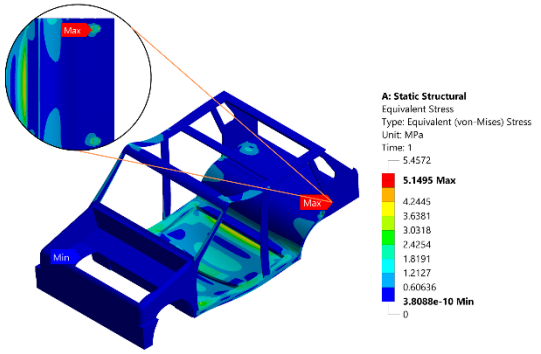

Fig. 13(d): *Low Alloy Steel.*

High strength steel shows the least deformation 0.097726 mm, emphasizing its suitability for this specific connection. The distinct total deformation values for other materials are as follows: Aluminum- 0.29935 mm, Low alloy steel - 0.15655 mm, Carbon fiber - 0.11927 mm (Figure 14).

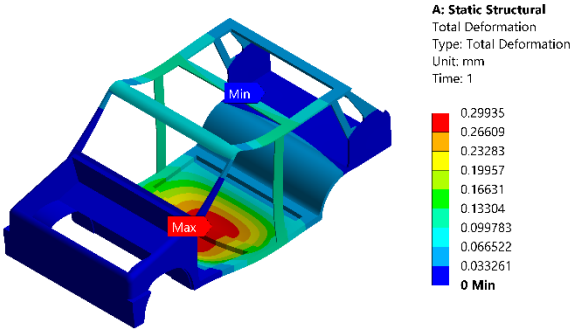

Fig. 14(a): *Aluminum.*

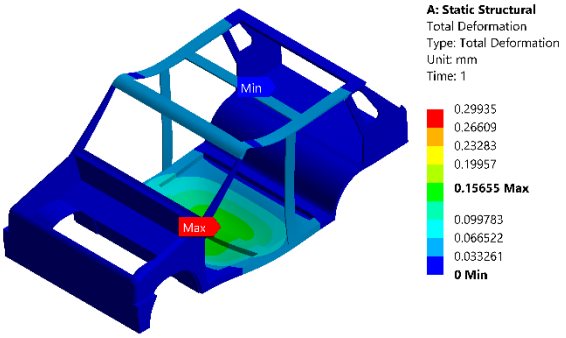

Fig. 14(b): *Carbon Fiber.*

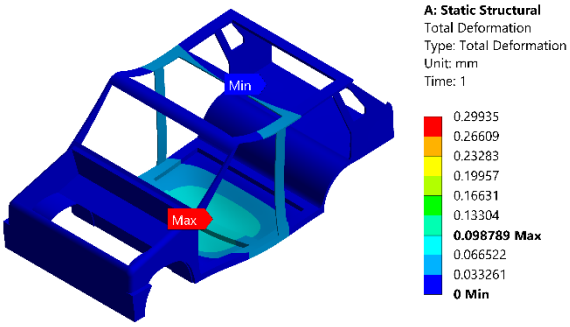

Fig. 14(c): High Strength Steel.

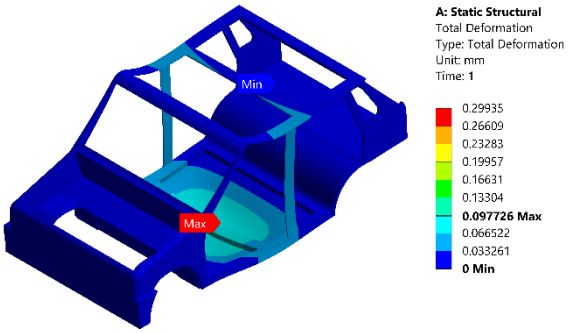

Fig. 14(d):. *Low Alloy Steel.*

4.4 Case IV: Motor at the Front and Battery in the Trunk

Examining the interaction between the battery trunk and motor front, aluminum leads with a maximum equivalent stress of 3.8079 MPa. High-strength steel follows with 4.5825 MPa, low alloy steel with 4.0748 MPa, and carbon fiber with 4.3184 MPa (Figure 15).

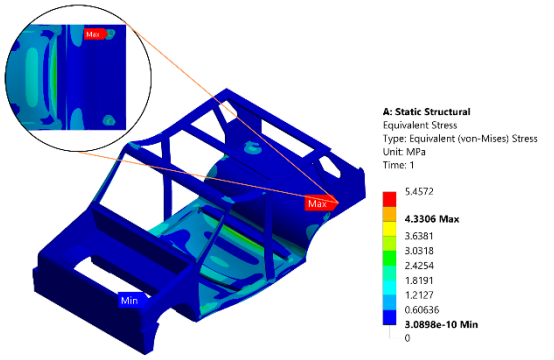

Fig. 15(a): *Aluminum.*

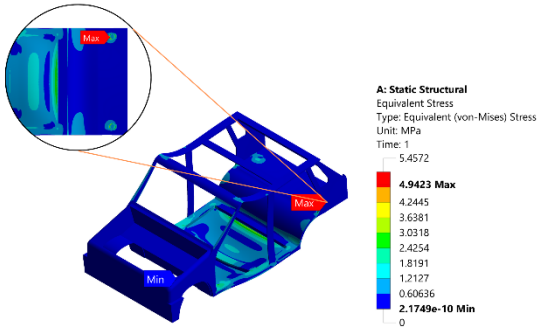

Fig. 15(b): *Carbon Fiber.*

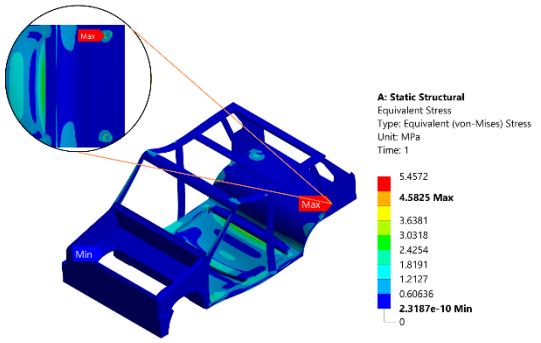

Fig. 15(c): *High Strength Steel.*

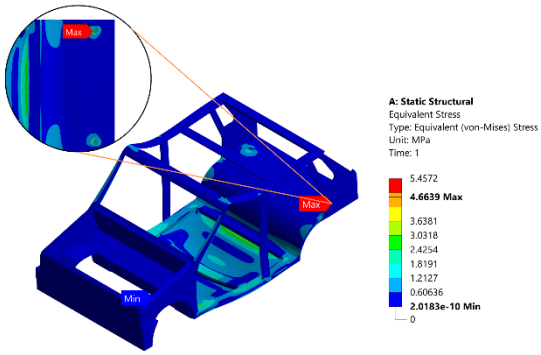

Fig. 15(d): *Low Alloy Steel.*

Low alloy steel shows the least deformation 0.075472 mm, showcasing its effectiveness in this specific structural scenario. The distinct total deformation values for other materials are as follows: High-strength steel -0.076289 mm, Aluminum - 0.23113 mm, Carbon fiber -0.12092 mm (Figure 16).

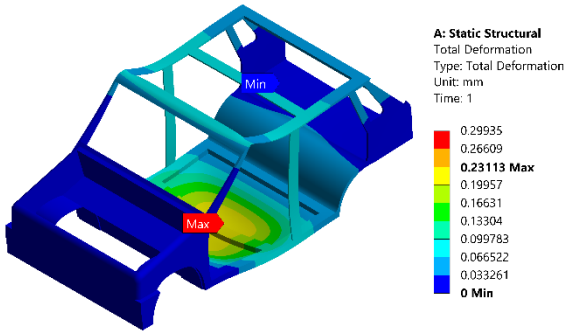

Fig. 16(a): *Aluminum.*

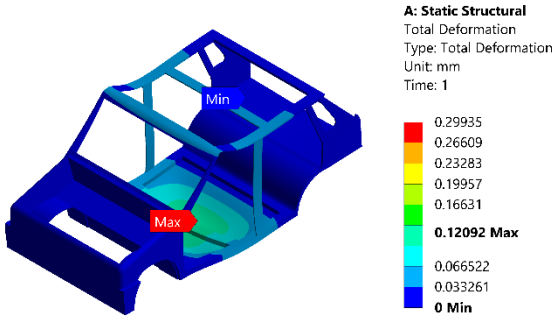

Fig. 16(b): *Carbon Fiber.*

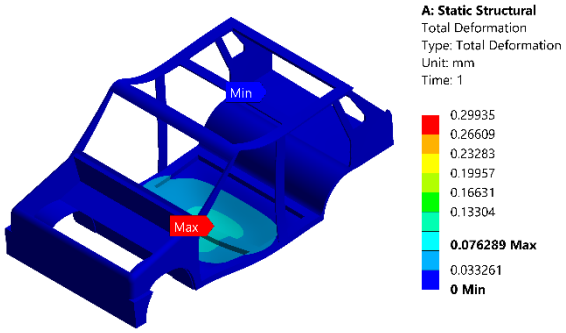

Fig. 16(c): *High Strength Steel.*

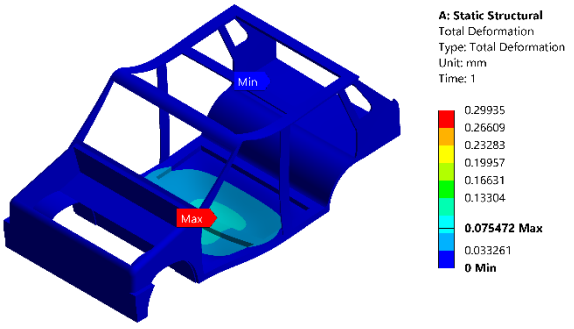

Fig. 16(d): *Low Alloy Steel.*

4.5 Case V: Motor at the Trunk and Battery at the Front

In the connection between the battery front and motor trunk, aluminum stands out with the highest stress levels numerically, reaching a maximum equivalent stress of 3.8079 MPa. High-strength steel follows with 4.0036 MPa, low alloy steel with 4.0748 MPa, and carbon fiber with 4.3184 MPa (Figure 17).

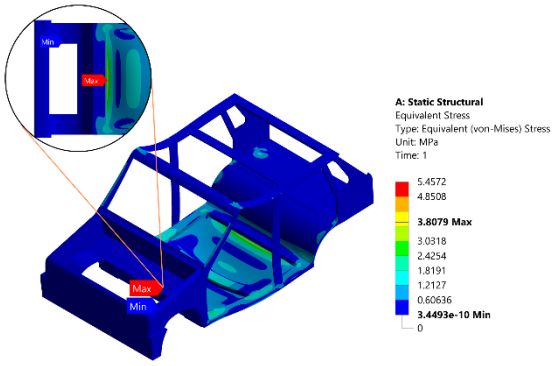

Fig. 17(a): *Aluminum.*

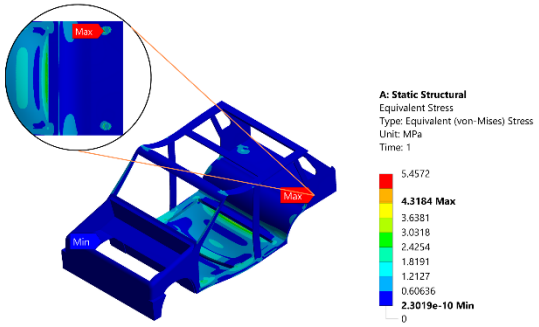

Fig. 17(b): *Carbon Fiber.*

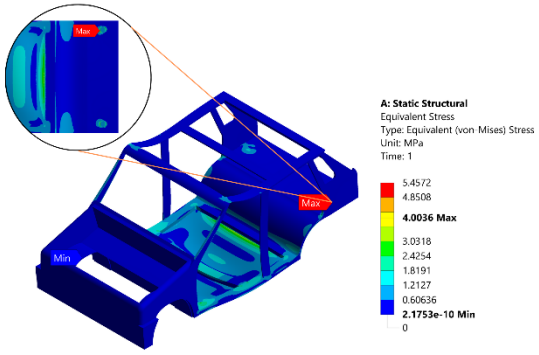

Fig. 17(c): *High Strength Steel.*

Low alloy steel shows the least deformation 0.074665 mm, emphasizing its structural suitability. The distinct total deformation values for other materials are as follows: High-strength

steel -0.075477 mm, Aluminum -0.2287 mm, Carbon fiber -0.11961 mm (Figure 18).

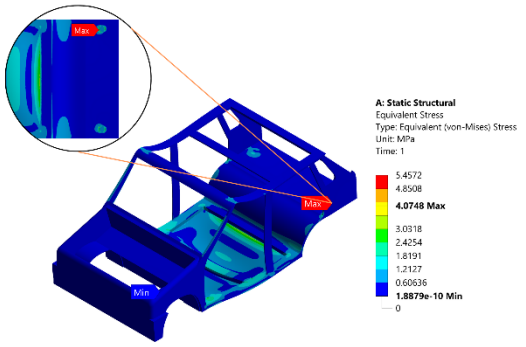

Fig. 17(d): *Low Alloy Steel.*

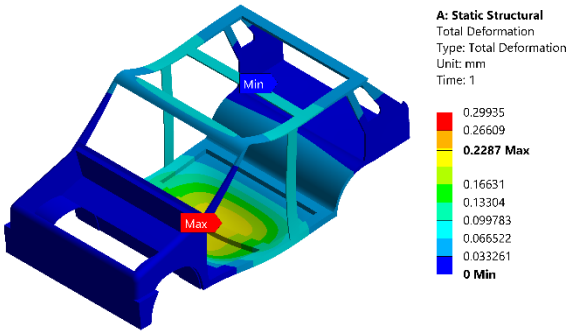

Fig. 18(a): *Aluminum.*

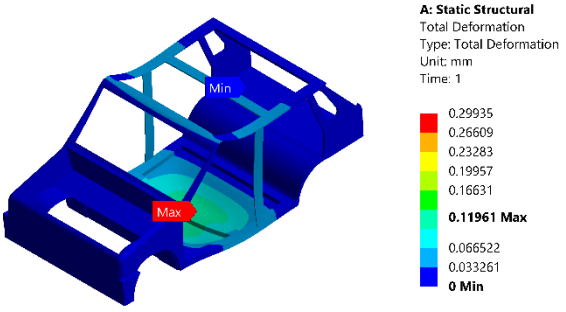

Fig. 18(b): *Carbon Fiber.*

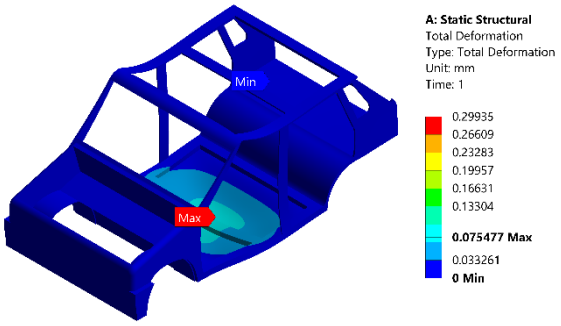

Fig. 18(c): *High Strength Steel.*

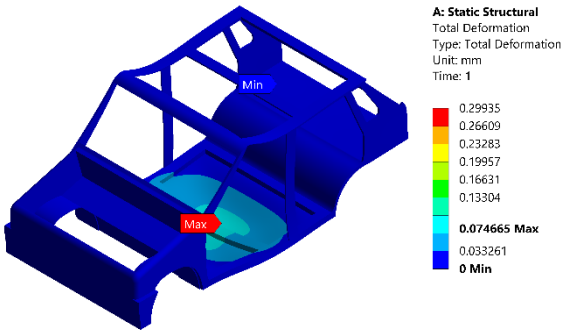

Fig. 18(d): *Low Alloy Steel.*

Table 7: shows the summary of the results.

Configuration	Maximum Equivalent Stress (MPa)	Maximum Deformation (mm)
Aluminium alloy, wrought 6061		
Case I	4.0748	0.22807
Case II	4.5694	0.23176
Case III	4.999	0.29935
Case IV	4.3306	0.23113
Case V	3.8079	0.2287
Carbon fibre		
Case I	4.1565	0.11927
Case II	5.1569	0.12127
Case III	3.4572	0.15655
Case IV	4.9423	0.12092
Case V	4.3184	0.11961
High strength steel		
Case I	3.8536	0.075265
Case II	4.8119	0.076503
Case III	5.0595	0.098787
Case IV	4.5825	0.076289
Case V	4.0036	0.075477
Low alloy normalized steel 4140		
Case I	3.9221	0.074455
Case II	4.8901	0.075685
Case III	5.1495	0.097726
Case IV	4.6639	0.075472
Case V	4.0748	0.074665

A consistent trend was seen where the least deformation and stress were observed when both the battery and motor were positioned in the front of the chassis. It suggests that the front placement configuration contributes to minimizing structural deformation and stress levels in the chassis under the applied load conditions. Figure

19 shows average values of stress, strain and deformation of every loading condition to check the strength of material. It is evident that low alloy steel emerges as the safest material due to its minimal deformation, while aluminum is comparatively weaker, displaying the highest deformation. When considering normalized equivalent stress, a lower value is favorable. Referring to Table 7, it becomes apparent that carbon fiber stands out as the safest material, as it exhibits the lowest normalized equivalent stress among the materials considered.

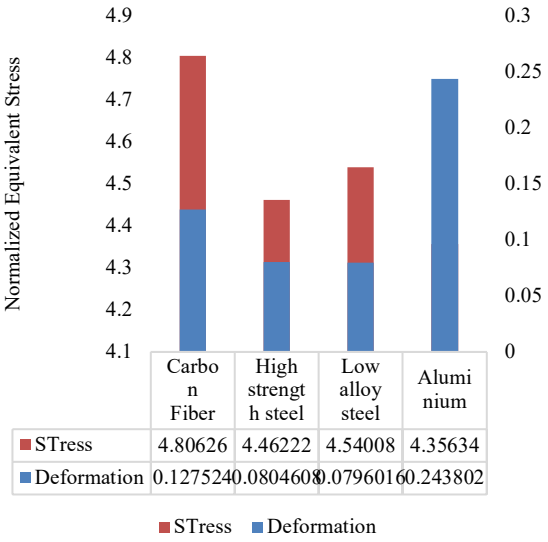

Fig.19: *Graph of material v/s stress*

5. CONCLUSION AND RECOMMENDDATIONS

Vehicle conversion requires comprehensive prior structural study to ensure stability. This study conducted static structural analysis in chassis of a conventional car model (Maruti 800) with electric retrofitting components. The car was modelled in SolidWorks and simulated in ANSYS. Variation in chassis material and placement of components were studied with pre-defined loads. The materials included carbon fiber, high-strength steel, low alloy normalized steel 4140, and aluminum alloy wrought 6061. A total load of 5,405.36 N was applied on different placement configurations of motor and battery: front, trunk, motor in front, battery in front, motor in trunk, battery in trunk, motor in front with battery at the bottom, and motor in trunk with battery in front. The ultimate stresses for the varied materials employed in this study for the chassis falls within the range of 3-12 MPa, all well below the allowable stress range of 104-1470 MPa. It can be inferred that the selected materials exhibit a high degree of safety for the structural integrity of the vehicle's chassis. Based on the simulation results, the optimal placement for the motor and battery is found to be at the front of the chassis. Additionally, low alloy steel stands out as the safest material choice for the chassis.

However, it is crucial to note that the conducted simulation was limited to static conditions. As a result, definitive conclusions regarding the specific material selection or optimal placement of the battery and motor cannot be made. Therefore, it is strongly recommended to extend this research into dynamic conditions through modal analysis to obtain a more comprehensive understanding and ensure the robustness of the chassis design in real-world and dynamic scenarios. Combining static and modal analysis will help create a robust design for a retrofitted vehicle. As Government of Nepal is taking initiatives to convert old internal combustion engine vehicles into electric to accelerate shift towards cleaner and sustainable transportation, this study is bound to serve as an important section of the guideline for conversion process, and also will promote industry practices that prioritize structural safety and sustainability.

6. REFERENCES

Volt Electric Scooter Speed Controllers - ElectricScooterParts.com. (n.d.). https://electricscooterparts.com/speedcontrollers72volt.html

AISI 4140 Alloy Steel: Fushun Special Steel Co., Ltd. - Professional Supplier of Special Steel, and Manufacturer of Tool Steel. (n.d.). https://www.fushunspecialsteel.com/aisi-4140-alloy-steel/

ANSYS SIMULATION SOFTWARE. (n.d.).

Ary, A. K., Prabowo, A. R., & Imaduddin, F. (2020). Structural assessment of alternative urban vehicle chassis subjected to loading and internal parameters using finite element analysis. *Journal of Engineering Science and Technology*, *15*(3), 1999–2022.

Balaguru, S., Natarajan, E., Ramesh, S., & Muthuvijayan, B. (2019). 6. *Materials Today: Proceedings*, *16*, 1106–1116. https://doi.org/10.1016/j.matpr.2019.05.202

Fully Isolated Heavy Duty Industrial and Military Grade 72VDC to 12VDC and 24VDC DC/DC Converters 40 Amp, 540 Watt. 5 year warranty. (n.d.). https://www.powerstream.com/dcdc-extreme-7212-500w.htm

GoN. (2016). First National Determined Contibution (NDC) Nepal. *Government of Nepal*, *2*(1), 38–41. https://doi.org/10.30852/sb.2012.38

GoN. (2020). Second Nationally Determined Contribution (NDC) Nepal. *Government of Nepal*, 0–21.

Government to allow conversion of ICE vehicles into electric or other alternative fuel vehicles. (2022, March). *Nepal Drives*.

Helal, M., Alogla, A., Abdel-aziz, K., Fouda, N., & Fathallah, E. (2018). Structure Topology Optimization of Internal Combustion Engine Connecting Rode Using Finite Element Analysis. *International Journal of Applied Engineering Research*, *13*(10), 7298–7304.

Journal, I., & Engineering, O. F. (2013). *11*. *2*(12).

LiFePO4 vs. Lithium Ion Batteries: What's the Best Choice for You? (n.d.). *EcoFlow US Blog*. https://blog.ecoflow.com/us/lifepo4-vs-lithium-ion-batteries/

Liu, M. B., Xie, W. P., & Liu, G. R. (2005). Modeling incompressible flows using a finite particle method. *Applied Mathematical Modelling*, *29*(12), 1252–1270. https://doi.org/10.1016/j.apm.2005.05.003

M.B. Liu a 1, W.P. Xie b, G. R. L. (n.d.). 7. *Modeling Incompressible Flows Using a Finite Particle Method*, *29*(12), 1252–1270. https://www.sciencedirect.com/science/article/pii/S0307904X0500096X#:~:text=FPM is a meshfree particle,through a sequence of transformations

maruti 800 tech detailing. (n.d.).

Mesh Quality: Mesh Visualization Tips. (n.d.). September 12, 2022. https://www.simscale.com/docs/simulation-setup/meshing/mesh-quality/

Nandhakumar, S., Seenivasan, S., Saalih, A. M., & Saifudheen, M. (2020). 5. *Materials Today: Proceedings*, *37*(Part 2), 1824–1827. https://doi.org/10.1016/j.matpr.2020.07.404

Ojha, A. (2018, February). countrywide Ban on Vehicle Older than 20 Yrs From March 15. *The Kathmandu Post*.

Permanent Magnet Synchronous Motor (PMSM) Contro. (n.d.). https://www.microchip.com/en-us/solutions/motor-control-and-drive/motor-types/permanent-magnet-synchronous-motors

Poudel, D., & Button, facebook sharing buttontwitter sharing. (2018). *2*. https://myrepublica.nagariknetwork.com/news/3-1-million-motor-vehicles-on-nepali-roads-dotm/

Prasain, K. (2024, February). EVs grab a third of auto import value. *The Kathmandu Post*.

Rajappan, R., & Vivekanandhan, M. (2013). 9. *The International Journal of Engineering and Science*, *2*(2), 63–73. www.theijes.com

Shiva Prasad, U., Babu, A. R., Sairaju, B., Amirishetty, S., & Deepak, D. (2020). Automotive chassis design material selection for road and race vehicles. *Journal of Mechanical Engineering Research and Developments*, *43*(3), 274–282.